CHAPTER IV

NOVEL BONE SCAFFOLDS BASED ON ELECTROSPUN POLYCAPROLACTONE FIBERS FILLED WITH CALCIUM CARBONATE OR HYDROXYAPATITE NANOPARTICLES: PREPARATION, CHARACTERIZATION, AND CYTOTOXICITY

SUMMARY

Novel bone scaffolding materials were successfully fabricated by electrospinning from polycaprolactone (PCL) solutions containing nanoparticles of calcium carbonate ($CaCO_3$) or hydroxyapatite (HA). The diameters of the as-spun fibers were found to increase with the addition and increasing amount of the nanoparticles. The observed increase in the diameters of the as-spun fibers with the addition and increasing amount of the nanoparticulate fillers was responsible for the observed increase in the tensile strength of the obtained fiber mats. An increase in the concentration of the base PCL solution caused the average diameter of the as-spun PCL/HA composite fibers to increase. Increasing applied electrical potential also resulted in an increase in the diameters of the obtained PCL/HA composite fibers. Lastly, indirect cytotoxicity evaluation of the electrospun mats of PCL, PCL/$CaCO_3$, and PCL/HA fibers based on human osteoblasts (SaOS2) and mouse fibroblasts (L929) revealed that these as-spun mats posed no threats to the cells, which, in turn, implied their potential utilization as bone scaffolding materials.

(**Key-words**: electrospinning; polycaprolactone; scaffold; cytotoxicity)

1. INTRODUCTION

Electrostatic spinning or electrospinning is an interesting method for producing non-woven fibers with diameters being in the range of sub-micrometers down to nanometers. In this process, a continuous filament is drawn from a polymer solution or melt through a spinneret by high electrostatic forces and later deposited on a grounded conductive collector.[1] Three main components for this technique are a high voltage power supply, a container for a polymer solution or melt with a small opening to be used as a nozzle, and a conductive collecting device. An emitting electrode of the power supply charges the polymer solution or melt by connecting the electrode to a conductive nozzle. Upon increasing the electrostatic field strength up to a critical value, charged species accumulated on the surface of a pendant drop destabilizes the partially-spherical into a conical shape (i.e. the Taylor cone). Beyond a critical value, a charged polymer jet is ejected from the apex of the cone and carried to the collector screen by the electrostatic force. The Coulombic repulsion force is responsible for the thinning of the charged jet during its flights to the collector. The charged jet elongates and, at the same time, dries out or solidifies to leave ultrafine fibers on the collector.

Due to high surface area to volume ratio of the electrospun fibers and high porosity in sub-micrometer length scale of the obtained non-woven mat, proposed applications for these materials are in areas such as nanofiber-reinforced composites, nanofiber-based supports for enzymes and catalysts, and nanofibrous membranes to be used in many biomedical applications,[2-5] including drug delivery, wound healing, and scaffolding for tissue engineering. The challenge in tissue engineering is the design of scaffolds that can mimic the structure and biological functions of the natural extracellular matrix (ECM). Electrospun fiber mats are uniquely suitable for uses as scaffolds because of their 3D structure with high porosity similar to fibrous collagen in natural ECM. The most commonly used synthetic polymers are polylactide (PLA), polyglycolide (PGA), polycaprolactone (PCL), and their corresponding co-polymers, due to their biodegradability and biocompatibility. PCL, due to its slow degradation rate, is a good candidate to be used in bone scaffolding applications. Electrospinning of PCL has been reported as successful from various

solvents.[5-8] Culture of chondrocytes and osteoblasts on neat electrospun PCL fibers has also been reported.[5,9] In addition, many researchers reported that incorporation of calcium carbonate ($CaCO_3$) or a type of calcium phosphate such as hydroxyapatite (HA) helped improve osteoblast proliferation and differentiation.[9-12]

In the present contribution, novel bone scaffolding materials from electrospun mats of PCL fibers filled with either $CaCO_3$ or HA nanoparticles were proposed. Among the various methods that have been used to synthesize HA nanoparticles,[13-16] hydrolysis[16] was simple and, therefore, chosen as the method for HA synthesis in this work. Morphological appearance, mechanical integrity, and cytotoxicity of the PCL composite fibrous scaffolds were characterized.

2. EXPERIMENTAL

2.1 Materials and synthesis and characterization of hydroxyapatite

Polycaprolactone (PCL; Aldrich, USA) has a number-average molecular weight of 80,000 g/mol. Dichloromethane (Carlo Erba, Italy) and *N,N*-dimethylformamide (DMF; Lab-Scan (Asia), Thailand) were used as solvents for PCL. Calcium carbonate nanoparticles ($CaCO_3$; average primary particle size = 40 nm) were donoted from NanoMaterials Technology (Singapore). Nano-sized hydroxyapatite (HA) powder was synthesized from dicalcium phosphate dihydrate ($CaHPO_4.2H_2O$; Fluka Chemika, Switzerland) by hydrolysis method following the procedure given in reference [16]. After hydrolysis, the HA powder was annealed at 800°C for 4 hr at a heating rate of 1°C/min in air. The obtained HA powder was characterized by a Rigaku Rint2000 wide-angle X-ray diffractometer (WAXD) using a monochromated CuK_α radiation (λ = 1.54 Å). Both morphology and size of the as-synthesized HA particles were characterized by a JEOL JSM 5410LV scanning electron microscope (SEM) and a MALVERN MastersizerX particle size analyzer, respectively, while size of the as-received $CaCO_3$ nanoparticulate power was examined with the same particle size analyzer.

2.2 Preparation and characterization of spinning dopes and electrospun fiber mats

Weighed amount of PCL pellets was dissolved in a mixed solvent of 50:50 v/v dichloromethane and DMF. To investigate the effect of filler content, either 0.5 or 1.0% w/v of $CaCO_3$ or HA powder was mixed in 12% w/v PCL solution. To investigate the effect of concentration of the base PCL solution, weighed amount of HA powder with the weight ratio between PCL and HA being 12:1 was mixed in 8, 10, or 12% w/v PCL solution. Prior to electrospinning, each of the spinning dopes was characterized for its viscosity, conductivity, and surface tension using a Brookfield DV-III programmable viscometer, an Orion 160 conductivity meter, and a KRÜSS DSA10-Mk2 drop-shape analyzer, respectively. All measurements were carried out at room temperature (i.e. 25 ± 1°C)

In electrospinning, each of the as-prepared spinning dopes was contained in a 50 ml glass syringe, the opening end of which was connected to a gauge 20 stainless steel needle (OD = 0.91 mm) used as the nozzle. A rotating drum (width and OD of the drum = 14 and 15 cm, respectively; rotational speed = 50 rpm) was used as a collector (see Figure 1). The outer surface of the rotating drum was set 10 cm from the tip of the needle. A Gamma High Voltage Research D-ES30PN/M692 power supply was used to generate a high DC potential. The applied potential used was 10, 15, or 21 kV and the polarity of the emitting electrode was positive, but, for experiments to investigate the effects of filler content and concentration of the base PCL solution, the applied potential was 21 kV. A Kd Scientific syringe pump was used to control the feed rate of the polymer solution at about 1 ml/h. As-spun fibers were dried *in vacuo* at 40°C overnight to remove as much solvent out as possible. Morphological appearance of the as-spun fibers was examined by SEM. Each sample was coated with a thin layer of gold using a JEOL JFC-1100E ion sputtering device prior to SEM observation. Diameters of the as-spun fibers were determined from SEM images using a SemAphore 4.0 software. For the above-mentioned experiments, the collection time was fixed at about 10 min.

2.3 Characterization and cytotoxicity of electrospun fibrous scaffolds

The electrospun fiber mats for potential use as scaffolding materials for bone regeneration were also characterized for their mechanical integrity and certain physical characteristics (i.e. average fiber diameter, average pore size, and porosity). These fibrous scaffolds were prepared under an applied electrostatic field strength of 21 kV/10 cm and the collection time of about 10 hr. The thickness of the resulting fiber mats was about 130 μm.

2.3.1 Mechanical and physical characteristics

Mechanical integrity in terms of yield stress and tensile strength was investigated using a Lloyd LRX universal testing machine (gauge length = 50 mm and crosshead speed = 10 mm/min). Mats of as-spun neat PCL and composite fibers were cut into a rectangular shape (10 mm × 70 mm). Average fiber diameter and average pore size of the fiber mats were examined by SEM. The average pore size was taken as an average of both the vertical and the horizontal dimensions of the pores. Lastly, porosity (ε) of the as-spun fibrous scaffolds was estimated based on the difference between the density of PCL (ρ_{PCL}) (i.e. about 1.145 g/cm^3) and the density of the mats (ρ_{sc}), according to the following equation:

$$\varepsilon(\%) = \left(1 - \frac{\rho_{sc}}{\rho_{PCL}}\right) \times 100 . \qquad (1)$$

The density of the fibrous scaffolds was measured by a Sartorius YDK01 density measurement kit.

2.3.2 Cytotoxicity testing

Two types of cells were used: 1) human osteoblasts (SaOS2) and 2) mouse fibroblasts (L929). Both cell types were cultured in Dulbecco's modified Eagle's medium (DMEM; Sigma-Aldrich, USA), supplemented by 10% fetal bovine serum (FBS; BIOCHROM AG, Germany), 1% L-glutamine (Invitrogen Corp., USA) and 1% antibiotic and antimycotic formulation [containing penicillin G sodium, streptomycin sulfate, and amphotericin B (Invitrogen Corp., USA)]. The cells were

re-plated once a week and cultures were maintained at 37°C in a humidified atmosphere containing 5% CO_2.

Indirect cytotoxicity test was conducted on fibrous scaffolds that were prepared from 12% w/v PCL solution and mixtures of 12% w/v PCL and 1.0% w/v $CaCO_3$ or 1.0% w/v HA, respectively, using the two mentioned cell lines. First, extraction media were prepared by immersing samples cut from the as-prepared fibrous scaffolds (about 15 mm in diameter and 130 μm in thickness) in wells of a 24-well culture plate in a serum-free medium (SFM; containing DMEM, 1% L-glutamine, 1 % lactabumin, and 1% antibiotic and antimycotic formulation) for 24 hr. Each of these extraction media was used to evaluate the cytotoxicity of the scaffolds. SaOS2 and L929 were separately cultured in wells of a 24-well culture plate in serum-containing DMEM for 16 hr to allow cell attachment on the plate. Then, the cells were starved with SFM for 24 hr, after which time the medium was replaced with an extraction medium. After 24 hr of cell culturing in the extraction medium, 3-(4,5-dimethylthiazol-2-yl)-2,5-diphenyl-tetrazolium bromide (MTT) assay was carried out to quantify the amount of viable cells.

The MTT assay is based on the reduction of the yellow tetrazolium salt to purple formazan crystals by dehydrogenase enzymes secreted from the mitochondria of metabolically active cells. The amount of purple formazan crystals formed is proportional to the number of viable cells. First, each culture medium was aspirated and replaced with 250 μl/well of MTT solution at 0.5 mg/ml for a 24-well culture plate. Secondly, the plate was incubated for 1 hr at 37°C. The solution was then aspirated and 900 μl/well of dimethylsulfoxide (DMSO) containing 125 μl/well of glycine buffer (pH = 10) was added to dissolve the formazan crystals. Finally, after 10 min of rotary agitation, the absorbance of the DMSO solution at 570 nm was measured using a Thermospectronic Genesis10 UV-visible spectrophotometer (Thermo Electron Corp., USA).

3. RESULTS AND DISCUSSION

3.1 Synthesis of hydroxyapatite (HA) and characterization of nanoparticles

Dicalcium phosphate dihydrate (DCPD; $CaHPO_4 \cdot 2H_2O$) is one of the precursors for the synthesis of HA. The hydrolysis of DCPD is based on the following reaction:

$$10CaHPO_4.2H_2O \rightarrow Ca_{10}(PO_4)_6(OH)_2 + 18H_2O + 12H^+ + 4PO_4^{3-}. \quad (2)$$

Although DCPD exhibits a low solubility in water, its hydrolysis reaction is a fast solid-solid phase transition occurring at a high pH value (>10) and temperature of about 60°C.[16] As a result, the solubility of DCPD in water is less important. A WAXD pattern of the as-synthesized HA powder after annealing at 800°C is shown in Figure 2. The average yield of HA was calculated to be about 90%. The peaks at the diffraction angles of about 26, 32, 33, and 53° corresponded to the (002), (300), (211), and (004) refraction planes of HA.[16,17] HA was reported[16] to crystallize in the hexagonal unit cell with axes $a = b = 9.418$ Å and $c = 6.884$ Å under $P6_3/m$ space group (JCPDS Card No. 9-432). The presence of other peaks suggested contamination of other phosphate compounds. For examples, the peaks at the diffraction angles of about 40 and 46° corresponded to $CaNaPO_4$.[17]

The morphology of the obtained HA powder was observed by SEM as shown in Figure 3. Both the primary and the secondary particles were evident. The size of the particles could be measured directly from SEM images and the average value was 234 ± 68 nm. On the other hand, result obtained from the particle size analyzer suggested a bimodel distribution in the size of the as-synthesized HA particles, with the lowest mean value being about 500 nm (see Figure 4). A rather wide distribution in the size of the as-received $CaCO_3$ particles was also suggested by the particle size analyzer. In this case, the lowest mean value of about 800 nm was obtained (result not shown). Since water was used as the medium to carry the particles pass the detector, the rather hydrophobic nature and the very small size of these particles should be the main cause for them to be present as large aggregates.

3.2 Electrospun PCL, PCL/$CaCO_3$, and PCL/HA fiber mats

Electrospinning of PCL has been successfully carried out in various solvents.[5-8] Lee and co-workers[6] found that electrospinability of PCL was enhanced when DMF was used as the co-solvent with dichloromethane, a direct result of the greater dielectric constant of DMF (i.e. 36.7[6]) in comparison with that of dichloromethane (i.e. 9.1[6]). In the present work, a 50:50 w/w mixture of dichloromethane and DMF was used as the solvent for the preparation of PCL solutions as well as PCL/$CaCO_3$ and PCL/HA mixtures for electrospinning.

3.2.1 Effect of filler content

Viscosity, conductivity, and surface tension for all of the as-prepared spinning dopes are summarized in Table 1. Evidently, the viscosity of the spinning dopes increased, while the conductivity decreased, from those of the neat PCL solution with the addition and increasing amount of both types of nanoparticles. Only the surface tension did not vary much. Einstein[18,19] pointed out long ago that the presence of non-interactive rigid particles increased the shear viscosity of dilute suspensions from that of pure liquid, while the presence of the non-conductive $CaCO_3$ and HA nanoparticles should intuitively decrease the conductivity of the resulting mixtures from that of the neat PCL solution.

Figure 5 shows selected SEM images of as-spun mats of neat PCL fibers and PCL fibers filled with $CaCO_3$ or HA nanoparticles of varying content. The concentration of the base PCL solution was 12% w/v and electrospinning was carried out at a fixed electrostatic field strength of 21 kV/10 cm for 10 min. Clearly, smooth fibers without the presence of beads were observed. At a slightly lower concentration (i.e. 10% w/v), beaded fibers were obtained (results not shown), a direct result of the low viscoelastic force in comparison with the Coulombic repulsion force.[20] Incorporation of both types of nanoparticles in the spinning dopes resulted in the formation of rough fibers. For as-spun neat PCL fibers, the average diameter was about 0.95 μm, while, for as-spun composite fibers, it ranged between 1.02 and 1.26 μm (see Table 1). Apparently, diameters of the as-spun composite

fibers increased with the addition and increasing amount of the filler. The observed increase in the fiber diameters of the composite fibers in comparison with those of the neat fibers should be a result of the observed increase in the viscosity of the spinning dopes due to the presence of the nanoparticles.

3.2.2 Effect of concentration of base PCL solution

The effect of the concentration of the base PCL solution on morphogical appearance and size of the as-spun fibers was investigated by mixing HA nanoparticles in a PCL solution of varying concentration (i.e. 8, 10, and 12% w/v). The weight ratio between PCL and HA was fixed at 12:1. According to Table 1, the viscosity of the spinning dopes increased, while both the conductivity and the surface tension decreased, with increasing concentration of the base PCL solutions. The significant increase in the viscosity of the spinning dopes with increasing concentration of the base PCL solutions was due to the increased molecular entanglement. Electrospinning of these spinning dopes was carried out at a fixed electrostatic field strength of 21 kV/10 cm for 10 min. Figure 6 shows selected SEM images of as-spun mats of PCL/HA fibers. Evidently, diameters of the obtained fibers increased with increasing concentration of the base PCL solutions, a direct result of the observed increase in the viscosity of the spinning dopes. The increased concentration enabled the charged jet to withstand larger stretching force (from the Coulombic repulsion).[20] Specifically, the average diameter of the obtained as-spun composite fibers increased from about 0.28 μm when the PCL concentration was 8% w/v to about 1.26 μm when the PCL concentration was 12% w/v (see Table 1).

3.2.3 Effect of applied potential

The effect of the applied potential on morphological appearance and size of the as-spun fibers was also investigated. A mixture of 12% w/v PCL and 1.0% w/v HA was electrospun under an applied potential of 10, 15, or 21 kV over a collection distance of 10 cm for 10 min. Smooth fibers without the presence of beads were obtained (results not shown), with the average diameter of the obtained as-spun composite fibers being 0.99 ± 0.02, 1.07 ± 0.02, and 1.26 ± 0.03 μm,

respectively. The obtained results indicated an increase in the fiber diameters with increasing applied potential, which could be a result of the increase in the mass throughput and/or the increase in the transport rate of the charged jet from the nozzle to the collector screen (due to the increase in the electrostatic force acting on the charged jet) that reduced the tendency for the charged jet to be thinned down by both the Coulombic repulsion force and the forces occuring during the bending instability.

3.3 Electrospun PCL, PCL/$CaCO_3$, and PCL/HA fibrous scaffolds

3.3.1 Mechanical and physical characteristics

To investigate the mechanical integrity of the fibrous scaffolds in terms of the yield stress and the tensile strength, the spinning dopes were electrospun continuously for 10 hr to obtain as-spun mats that were about 130 μm in thickness. The obtained fibrous scaffolds were physically similar to the fiber mats that were collected over a much shorter time period (i.e. 10 min) (see Figure 5) in terms of both the diameters and the randomness of the fibers within the mats. The yield strength of the neat scaffold was about 2.8 MPa, while that of the composite scaffolds was greater than that of the neat one, with the property value ranging between about 3.6 and 3.9 MPa (see Table 1). Interestingly, the observed increase in the tensile strength at yield with the addition and increasing amount of both types of nanoparticles was in accord with the observed increase in the fiber diameters (see Table 1). With regards to the yield stress, most of the composite scaffolds exhibited the property value lower than that of the neat one, excepted for the one that was filled with 0.5% w/v $CaCO_3$ (see Table 1). In addition, the average pore size and the porosity of the fibrous scaffolds were carefully investigated and the results are also summarized in Table 1. Apparently, the average pore size of the scaffolds ranged from about 4.3 to 5.6 μm. The highly porous nature of these fibrous scaffolds is quickly recognized when their porosity was estimated to range between about 82 and 90%.

3.3.2 Cytotoxicity

Indirect cytotoxicity test was conducted on fibrous scaffolds that were prepared from 12% w/v PCL solution and mixtures of 12% w/v PCL and 1.0% w/v $CaCO_3$ or 1.0% w/v HA, respectively, using SaOS2 and L929 cell lines. Even though we were interested in using the obtained fiber mats as potential bone scaffolds, it was mandatory to test the materials with L929 just to comply with the ISO10993-5 standard test method. Figure 7 shows the absorbance obtained from MTT assay of the cells which were cultured with the extraction media in comparison with those cultured with SFM (i.e. control). Evidently, for SaOS2, PCL and PCL/HA fibrous scaffolds exhibited comparable average absorbance values, while PCL/$CaCO_3$ fibrous scaffold exhibited a slightly lower average absorbance value, in comparison with that of the control. On the other hand, for L929, all of the fibrous scaffolds exhibited much greater average absorbance values in comparison with that of the control, with that of the PCL/HA fibrous scaffold being the greatest, followed by that of the PCL/$CaCO_3$ one. All of the obtained results clearly suggested that electrospun mats of PCL and PCL fibers filled with either $CaCO_3$ or HA nanoparticles were non-toxic to both types of cells and posed as good candidates to be used as bone scaffolds.

4. CONCLUSIONS

In the present contribution, electrospinning was used to fabricate novel bone scaffolding materials from electrospun mats of polycaprolactone (PCL) filled with either calcium carbonate ($CaCO_3$) or hydroxyapatite (HA) nanoparticles. HA was successfully synthesized by hydrolysis method, with the average particle size based on visual observation being about 230 nm. The viscosity of the spinning dopes increased with the addition and increasing amount of the nanoparticles, which, in turn, was postulated to be the main reason for the observed increase in diameters of the as-spun fibers. The observed increase in the diameters of the as-spun fibers with the addition and increasing amount of the nanoparticulate fillers was likely responsible for the observed improvement in the tensile strength of the obtained fiber mats. The concentration of the base PCL solution had a strong effect on the size of

the as-spun fibers, in which the average diameter of the as-spun PCL/HA composite fibers was found to increase with increasing concentration of the base PCL solutions. Increasing applied electrical potential also resulted in an increase in the diameters of the obtained PCL/HA composite fibers. Lastly, the applicability for the electrospun mats of PCL, PCL/$CaCO_3$, and PCL/HA fibers to be used as bone scaffolds was evaluated by an indirect cytotoxicity test using human osteoblasts (SaOS2) and mouse fibroblasts (L929) as reference cells. The results suggested a high potential for use of these fiber mats as bone scaffolds and it is expected that the scaffold made from electrospun PCL/HA composite fibers should be the best among the three systems investigated, because of the known ability of HA to promote bone cell activities.

ACKNOWLEDGEMENTS

The authors acknowledge partial support received from the National Research Council of Thailand, Chulalongkorn University (through invention and research grants from the Ratchadapesek Somphot Endowment Fund), the Petroleum and Petrochemical Technology Consortium [through a Thai governmental loan from Asian Development Bank (ADB)], and the Petroleum and Petrochemical College (PPC), Chulalongkorn University. PS acknowledges Thailand Toray Science Foundation for a Science and Technology Research Grant in 2004 and PW acknowledges a doctoral scholarship received from the Development and Promotion of Science and Technology Talents Project, the Institute for the Promotion of Teaching Science and Technology.

REFERENCES

[1] US Patent 1,975,504 (1934), inv.: A. Formhals.

[2] E. R. Kenawy, G. L. Bowlin, K. Mansfield, J. Layman, D. G. Simpson, E. H. Sanders, G. E. Wnek, *Journal of Controlled Release* **2002**, *81*, 57.

[3] B. M. Min, L. Jeong, Y. S. Nam, J. M. Kim, W. H. Park, *International Journal of Biological Macromolecules* **2004**, *34*, 281.

[4] H. Yoshimoto, Y. M. Shin, H. Terai, J. P. Vacanti, *Biomaterials* **2003**, *24*, 2077.

[5] W. J. Li, R. Tuli, C. Okafor, A. Derfoul, K. G. Danielson, D. J. Hall, R. S. Tuan, *Biomaterials* **2005**, *26*, 599.

[6] K. H. Lee, H. Y. Kim, M. S. Khil, Y. M. Ra, D. R. Lee, *Polymer* **2003**, *44*, 1287.

[7] M. Shin, O. Ishii, T. Sueda, J. P. Vacanti, *Biomaterials* **2004**, *25*, 3717.

[8] S. A. Theron, E. Zussman, A. L. Yarin, *Polymer* **2004**, *45*, 2017.

[9] K. Fujihara, M. Kotaki, S. Ramakrishna, *Biomaterials* **2005**, *26*, 4139.

[10] D. Turhani, B. Cvikl, E. Watzinger, M. Weizenhock, K. Yerit, D. Thurnher, G. Lauer, R. Ewers, *Journal of Oral and Maxillofacial Surgery* **2005**, *63*, 793.

[11] A. G. A. Coombes, S. C. Rizzi, M. Williamson, J. E. Barralet, S. Downes, W. A. Wallace, *Biomaterials* **2004**, *25*, 315.

[12] S. Maeno, Y. Niki, H. Matsumoto, H. Morioka, T. Yatabe, A. Funayama, Y. Toyama, T. Taguchi, J. Tanaka, *Biomaterials* **2005**, *26*, 4847.

[13] C. Li-yun, Z. Chuan-bo, H. Jian-feng, *Materials Letters* **2005**, *59*, 1902.

[14] G. Guo, Y. Sun, Z. Wang, H. Guo, *Ceramics International* **2005**, *31*, 869.

[15] Y. X. Pang, X. Bao, *Journal of the European Ceramic Society* **2003**, *23*, 1697.

[16] W. J. Shih, Y. F. Chen, M. C. Wang, M. H. Hon, *Journal of Crystal Growth* **2004**, *270*, 211.

[17] M. Wei, J. H. Evans, T. Bostrom, L. Grondahl, *Journal of Material Science: Materials in Medicine* **2003**, *14*, 311.

[18] A. Einstein, *Annual Physics* **1906**, *19*, 289.

[19] A. Einstein, *Annual Physics* **1911**, *34*, 591.

[20] C. Mit-uppatham, M. Nithitanakul, P. Supaphol, Macromolecular Chemistry and Physics **2004**, *205*, 2327.

CAPTION OF FIGURES

Figure 1 Schematic diagram of electrospinning setup.

Figure 2 Wide-angle X-ray diffraction pattern of as-synthesized hydroxyapatite (HA) powder.

Figure 3 Selected scanning electron micrograph of as-synthesized HA powder.

Figure 4 Size distribution of as-synthesized HA powder as analyzed by particle size analyzer.

Figure 5 Selected scanning electron micrographs of as-spun fibers from (a) 12% w/v PCL, (b) 12% w/v PCL with 0.5% w/v $CaCO_3$, (c) 12% w/v PCL with 1.0% w/v $CaCO_3$, (d) 12% w/v PCL with 0.5% w/v HA, (e) 12% w/v PCL with 1.0% w/v HA. The applied electrostatic field strength was 21 kV/10 cm and the collection time was 10 min.

Figure 6 Selected scanning electron micrographs of as-spun fibers from (a) 8% w/v PCL with 0.67% w/v HA, (b) 10% w/v PCL with 0.83% w/v HA, and (c) 12% w/v PCL with 1.0% w/v HA. The applied electrostatic field strength was 21 kV/10 cm and the collection time was 10 min.

Figure 7 Indirect cytotoxic evaluation of fibrous scaffolds from electrospun mats of neat PCL fibers and PCL fibers filled with $CaCO_3$ or HA nanoparticles based on viability of human osteoblasts (SaOS2) and mouse fibroblasts (L929).

SHORT TEXT FOR TABLE OF CONTENTS

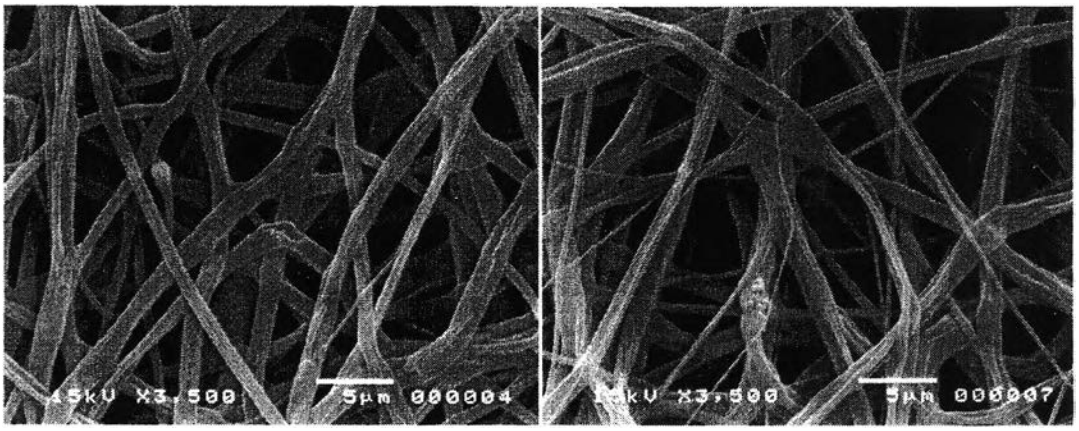

Selected scanning electron micrographs of electrospun fibers from 12% w/v polycaprolactone solution filled with either 1.0% w/v calcium carbonate (left) or 1.0% w/v hydroxyapatite (right) nanoparticles. Indirect cytotoxicity evaluation of these electrospun mats based on both human osteoblasts (SaOS2) and mouse fibroblasts (L929) supported their potential use as bone scaffolding materials.

Table 4.1 Some important properties of as-prepared spinning drops, average diameter of the resulting electrospun fibers, and mechanical integrity and some important characteristics of the resulting electrospun fiber mats

Sample/ Properties	12% PCL	12% PCL/0.5% $CaCO_3$	12% PCL/1.0% $CaCO_3$	12% PCL/0.5% HA	12% PCL/1.0% HA	10% PCL/0.83% HA	8% PCL/0.67% HA
Viscosity (cp)	447	552	591	487	550	348	280
Conductivity (μs/cm)	5.0	4.0	3.4	3.3	3.1	3.4	3.9
Surface tension (mN/m)	29.5	29.1	28.5	29.2	28.1	29.8	29.9
Average fiber diameter (μm)	0.95 ± 0.02	1.02 ± 0.03	1.12 ± 0.03	1.24 ± 0.03	1.26 ± 0.03	0.42 ± 0.02	0.28 ± 0.02
Yield stress (MPa)	2.40 ± 0.45	2.67 ± 0.54	2.25 ± 0.36	2.15 ± 0.23	2.20 ± 0.27	n/a	n/a
Tensile strength (MPa)	2.84 ± 0.51	3.63 ± 0.50	3.76 ± 0.94	3.77 ± 0.14	3.93 ± 0.05	n/a	n/a
Average pore size (μm)	5.57 ± 2.53	4.80 ± 1.97	4.28 ± 1.86	4.79 ± 2.29	5.35 ± 2.52	n/a	n/a
Porosity (%)	85.8 ± 5.1	89.2 ± 3.1	90.4 ± 2.8	81.6 ± 5.6	82.4 ± 4.4	n/a	n/a

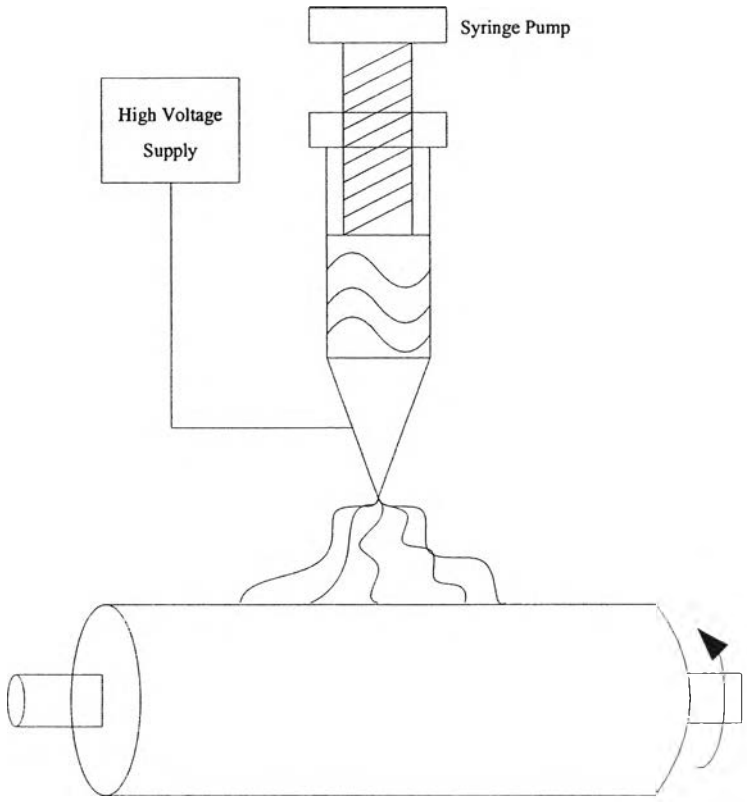

Figure 4.1 Schematic diagram of electrospinning setup.

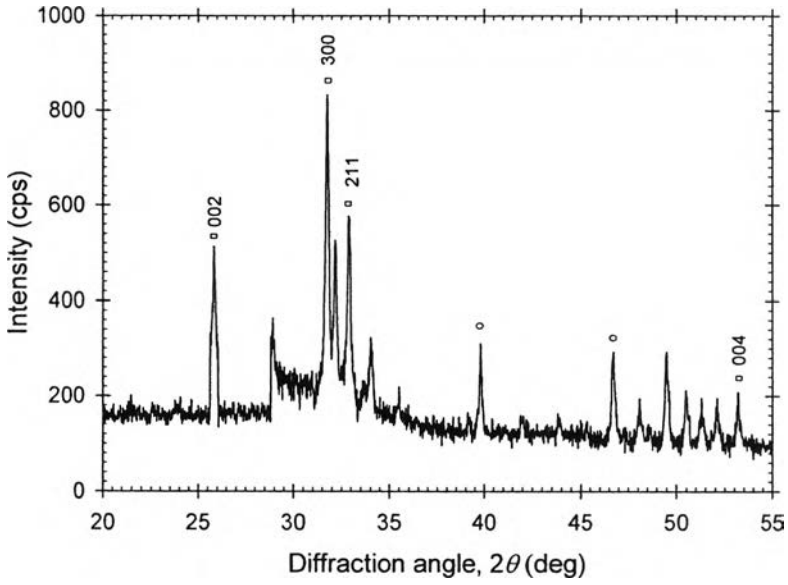

Figure 4.2 Wide-angle X-ray diffraction pattern of as-synthesized hydroxyapatite (HA) powder.

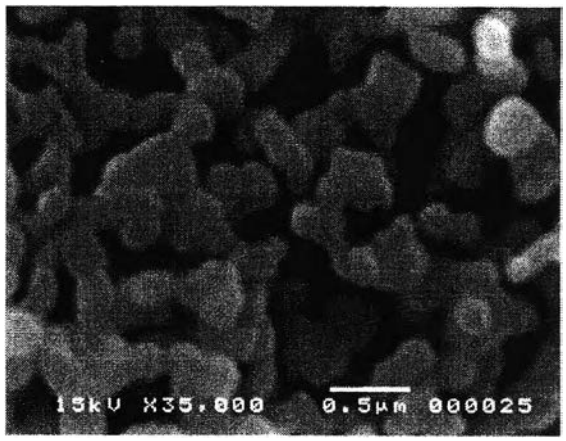

Figure 4.3 Selected scanning electron micrograph of as-synthesized HA powder.

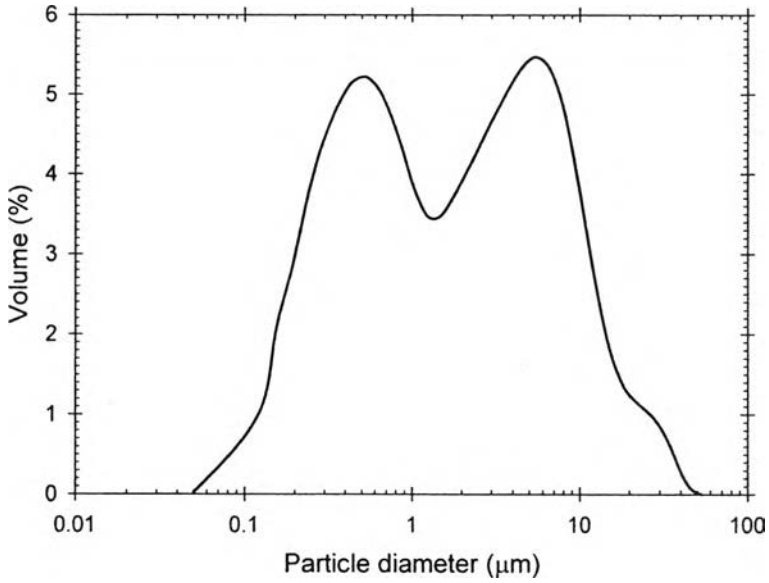

Figure 4.4 Size distribution of as-synthesized HA powder as analyzed by particle size analyzer.

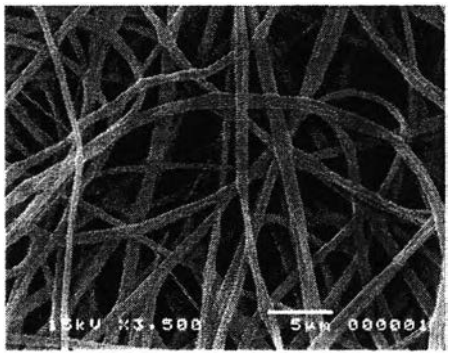

(a)

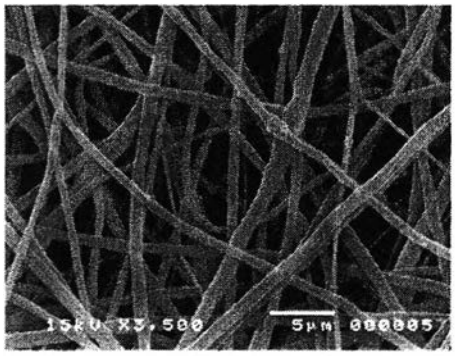

(b)

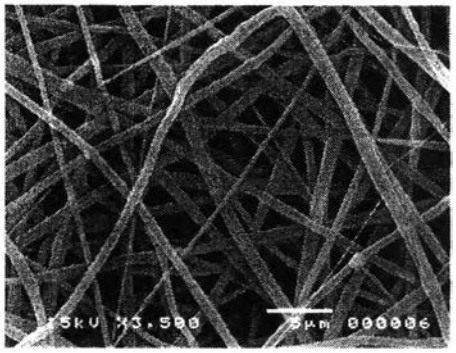

(d)

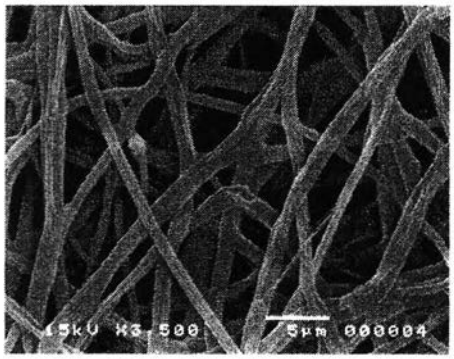

(c)

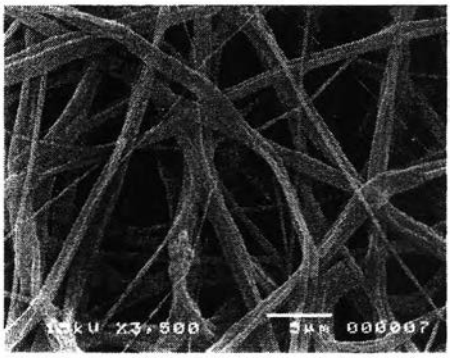

(e)

Figure 4.5 Selected scanning electron micrographs of as-spun fibers from (a) 12% w/v PCL, (b) 12% w/v PCL with 0.5% w/v $CaCO_3$, (c) 12% w/v PCL with 1.0% w/v $CaCO_3$, (d) 12% w/v PCL with 0.5% w/v HA, (e) 12% w/v PCL with 1.0% w/v HA. The applied electrostatic field strength was 21 kV/10 cm and the collection time was 10 min.

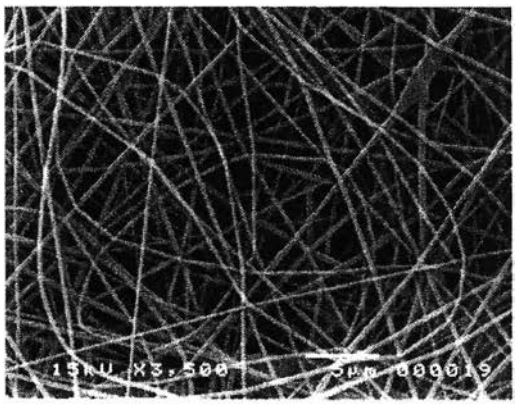

(a)

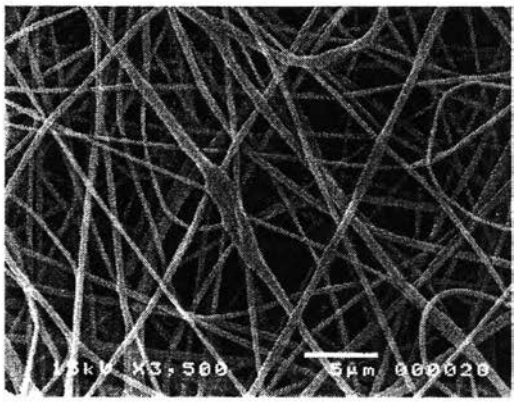

(b)

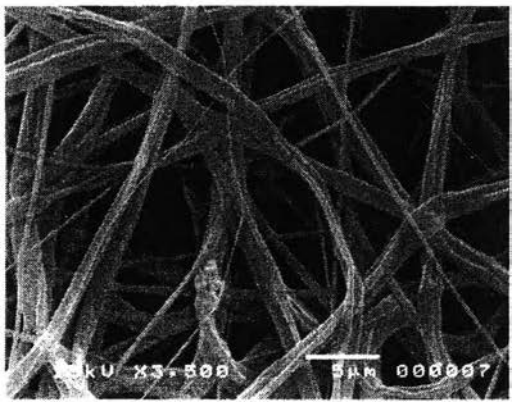

(c)

Figure 4.6. Selected scanning electron micrographs of as-spun fibers from (a) 8% w/v PCL with 0.67% w/v HA, (b) 10% w/v PCL with 0.83% w/v HA, and (c) 12% w/v PCL with 1.0% w/v HA. The applied electrostatic field strength was 21 kV/10 cm and the collection time was 10 min.

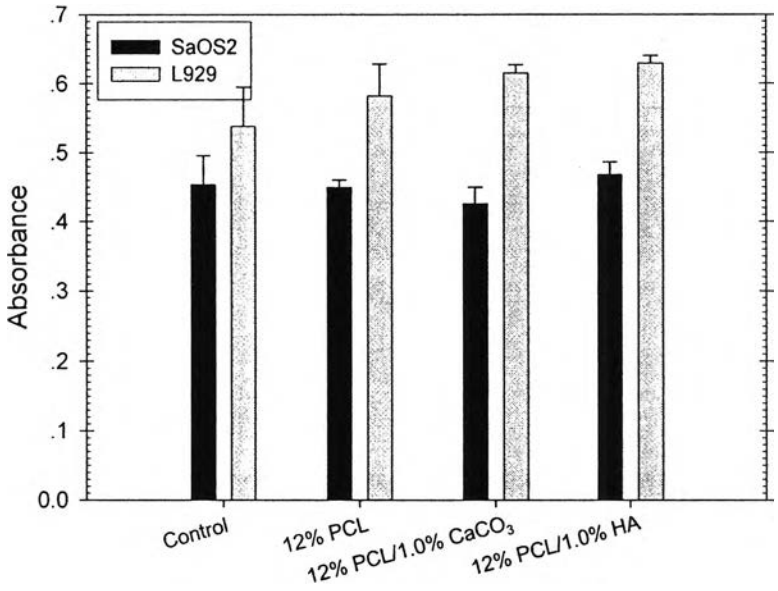

Figure 4.7 Indirect cytotoxic evaluation of fibrous scaffolds from electrospun mats of neat PCL fibers and PCL fibers filled with $CaCO_3$ or HA nanoparticles based on viability of human osteoblasts (SaOS2) and mouse fibroblasts (L929).